

IMECE2012-87174

A COUPLED TRANSPORT AND SOLID MECHANICS FORMULATION FOR MODELING OXIDATION AND DECOMPOSITION IN A URANIUM HYDRIDE BED

Maher Salloum

Sandia National Laboratories
Livermore, CA, USA

Mike Kanouff

Sandia National Laboratories
Livermore, CA, USA

Andrew Shugard

Sandia National Laboratories
Livermore, CA, USA

Patricia Gharagozloo

Sandia National Laboratories
Livermore, CA, USA

ABSTRACT

Modeling of reacting flows in porous media has become particularly important with the increased interest in hydrogen solid-storage beds. It is important for design applications to have an accurate, but relatively simple model for system analysis. We are interested in simulating the reaction of uranium hydride and oxygen gas in a hydrogen storage bed using multiphysics finite element modeling. Our model considers chemical reactions, heat transport, and mass transport within a hydride bed. Previously, the time-varying permeability and porosity were considered uniform. This led to discrepancies between the simulated results and experimental measurements. In this work, we account for the effects of non-uniform changes in permeability and porosity due to phase and thermal expansion. These expansions result in mechanical stresses which lead to bed deformation. To describe this, we develop a simplified solid mechanics model for the local variation of permeability and porosity as a function of the local bed deformation. We find that, by using this solid mechanics model, we improve the agreement between our reacting bed model and the experimental data.

INTRODUCTION

Uranium hydride powder beds have been used extensively for hydrogen isotope storage (1-3). Uranium hydride is pyrophoric (4-7) and therefore air ingress accidents have been a longstanding concern. Given sufficient air or oxygen, high temperatures can be reached within the bed, leading to hydride decomposition, which produces hydrogen gas. Hydrogen gas release is undesirable

in an accident scenario. Alternatively however, injecting oxygen into a uranium hydride bed could be an effective way to quickly generate hydrogen gas for small devices such as portable fuel cells (8). A mathematical model is extremely useful when designing an optimal hydrogen generating reactor. Such a model could also be used to predict the outcome of storage bed air ingress accidents.

A detailed numerical model of oxidation and decomposition in a uranium hydride bed was recently developed by Kanouff *et al.* (9). The model explicitly considers rates of chemical reaction, heat transport, and mass transport within the porous bed. The model was developed for comparison to experiments described by Shugard *et al.* (8). In Kanouff's model, it was assumed that a mechanical equilibrium exists within the bed such that the porosity is uniform; and therefore only a function of the mean bed composition. The hydraulic permeability is recovered from the mean porosity using Young's law (10); such that it is also uniform within the bed. Comparisons with Shugard *et al.*'s measurements show this to be a reasonably effective approximation (9). However, discrepancies in the pressure and temperature response of the hydride bed suggest that the permeabilities computed by this simplified model are not entirely accurate.

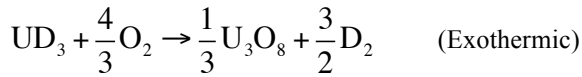
In this study, we relax the uniform porosity assumption by computing a porosity field within the bed. The local permeability is then recovered using Young's law, similar to Kanouff's model. The thermal and phase expansions occurring in the bed induce deformations that, in turn, result in changes in the local porosity. We quantify these deformations using a solid mechanics model. A simplified linear elastic model is developed to describe bed

deformation inside the closed reactor volume. We couple this solid mechanics model to Kanouff *et al.*'s transport model. Below we present the extended model, apply it to two oxygen injection cases previously simulated by Kanouff *et al.*, and compare the results. We find that, by coupling the solid mechanical and transport models, we improve the agreement between simulated and measured bed response.

SOLID MECHANICS MODEL FORMULATION

We develop a solid mechanics model based on the reactor geometry described by Shugard *et al.*, (8), and depicted in Figure 1. The reactor is axisymmetric and is divided into four sub-domains: the oxygen (O₂) source and flow channels (Ω₁), the reactor bed (Ω₂), the frits at the reactor entrance and exit (Ω₃), and the reactor stainless steel housing (Ω₄). We develop our model using uranium deuteride (UD₃) because Shugard *et al.*, (8), used UD₃ instead of UH₃ because the resulting deuterium gas is easier to detect.

As O₂ is injected, a reaction front forms leading to the formation of uranium (U) and uranium oxide (U₃O₈), as depicted in Figure 1 (right). The oxidation and decomposition of UD₃ are assumed to be governed by the following chemical reactions:



Additional details about the chemical reactions, model geometry and mathematical formulation can be found in (8-9).

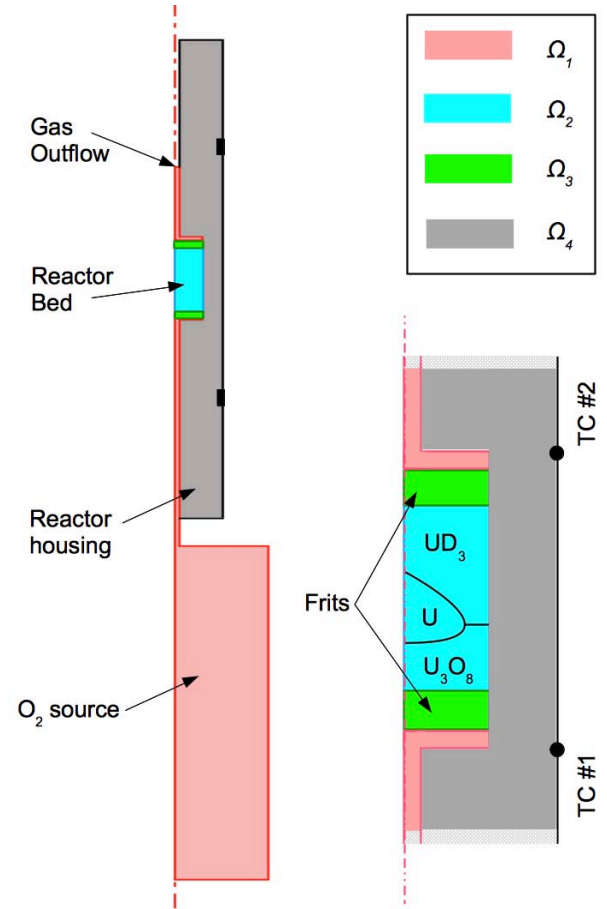


Figure 1: A schematic of the axisymmetric reactor model. The schematic shows: (left) the entire model domain, comprised of the O₂ source and flow channels (Ω₁), the UD₃ reactor bed (Ω₂), the frits at the reactor entrance and exit (Ω₃), and the reactor stainless steel housing (Ω₄); and (right) a magnified view of the reactor depicting typical species distribution during the reaction. The temperature is monitored in the experiments at two locations TC#1 and TC#2 at the reactor housing outer surface.

The consumption and formation of different solid species within the reactor bed induces phase and thermal strain. Because the reactor is closed, these local strains generate stresses, which are transferred to unreacted regions of the bed, causing further deformation. We describe these stresses and deformations using a solid mechanics model. The differential equations governing the stresses are assumed to apply only in the reactor bed domain Ω₂. A quasi-static equilibrium is assumed within the bed; and therefore:

$$\nabla \cdot [\sigma] = 0 \quad (1)$$

where [σ] is the stress matrix. The boundaries of Ω₂ are assumed to be frictionless, rigid, walls. Assuming linear-elastic and isotropic behavior for the U, UD₃ and U₃O₈ powders, local stress and strain are related by:

$$[\epsilon^e] = \frac{1+\nu}{E} [\sigma] - \frac{\nu}{E} \text{Tr}([\sigma]) [I] \quad (2)$$

where E and ν are the elastic modulus and Poisson's ratio respectively, $[\epsilon^e]$ is the elastic strain, $Tr([\sigma])$ is the trace of $[\sigma]$, and $[I]$ is the identity matrix. E and ν were obtained from (11-13) for the different phases, as a function of temperature. Assuming the powders behave as linear-elastic solids greatly oversimplifies their behavior; which is better described as elastic-plastic (14). We selected a linear-elastic formulation because it is numerically tractable.

The total strain is given by the sum of the elastic strain, Eq. 2, and the strain due to the thermal and phase expansions. The total strain $[\epsilon]$ is:

$$[\epsilon] = [\epsilon^e] + [\epsilon^{th}] + [\epsilon^{ph}] \quad (3)$$

where $[\epsilon^{ph}]$ and $[\epsilon^{th}]$ are the strains due thermal and phase expansion respectively. They are:

$$[\epsilon^{th}] = \alpha \Delta T [I] \quad (4)$$

$$[\epsilon^{ph}] = \sum_{i=U_3O_8, U} \frac{\Delta V_i}{3} x_i [I] \quad (5)$$

where α is the thermal expansion coefficient, ΔT is the temperature elevation, ΔV is the phase expansion relative to UD_3 and x is the mole fraction of solid species i . Thermal expansion coefficients were obtained from (15-16) for the different species. For U_3O_8 and U , ΔV are 0.536 and -0.432 respectively.

Solving Eqs. 1-5 gives the total strain $[\epsilon]$. The volumetric expansion e is given by the trace of $[\epsilon]$:

$$e = Tr([\epsilon]) \quad (6)$$

The local porosity ϕ is then computed using:

$$\phi = 1 - \frac{(1 - \phi_0) \left(1 + \sum_{i=U_3O_8, U} \Delta V_i x_i \right)}{1 + e} \quad (7)$$

where $\phi_0=0.605$ is the initial (UD_3) bed porosity. In Eq. 7 the $(1+e)$ term accounts for local volumetric expansion or contraction of the porous element; while the

$(1 - \phi_0) \left(1 + \sum_{i=U_3O_8, U} \Delta V_i x_i \right)$ term accounts for phase expansion within the element.

Finally, the local bed permeability, κ , is recovered using Young's law (10):

$$\kappa = \frac{\phi d_p^2}{\tau^2} \left(\frac{1}{32} + \frac{5}{12} Kn \right) \quad (8)$$

where Kn is the local Knudsen number, τ is the tortuosity and d_p is the characteristic pore size. The bed parameters τ and d_p are calculated from experimental calibrations described in Shugard *et al.* (8).

This solid mechanics model is coupled to Kanouff's transport model, (9), and solved using the finite element method (COMSOL Multiphysics 3.5a). In some cases, the local bed deformation is comparable to the element size. Therefore our solution uses a total Lagrangian formulation (17).

RESULTS AND DISCUSSION

The model was used to simulate two O_2 injection experiments (O_2 injection #1 and #2). These experiments were carried out successively on a single reactor. In O_2 injection #1, only a small amount of O_2 was injected resulting in partial oxidation of the hydride material. In O_2 injection #2, a larger amount of O_2 was injected into the same reactor, but still leaving about 60% of the hydride material unreacted (8).

O_2 injection #1

During injection 1, 15% of the O_2 required to fully oxidize the bed to U_3O_8 was slowly injected over about 300 seconds. The O_2 was released from a source bottle initially at 20 psia. As the O_2 flows slowly into the bed, the reaction raised the local temperature to about 100 °C; as shown in *Figure 2(a)*. This temperature is low enough that the upstream region of the bed oxidizes without causing noticeable UD_3 decomposition. The temperature increase and oxidation induce volumetric expansions in the upstream portion of the bed, both of which decrease the local porosity; this is depicted in *Figure 2(c)*.

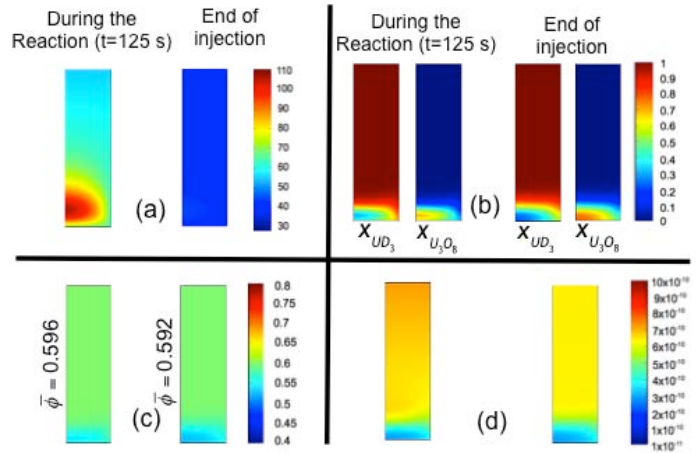


Figure 2: Plots of the (a) temperature (°C), (b) composition, (c) porosity, and (d) permeability (cm^2), inside the bed for O_2 injection #1. The plots are generated during the reaction ($t=125$ s) and at the end of the injection, as indicated.

The expanding region compresses the unreacted UD_3 powder such that the porosity is decreased on average. This is consistent with the model of Kanouff *et al.* (8-9) where it

was shown that the uniform porosity decreases as the reaction progresses. The predicted and measured pressure decays in the O₂ source vessel are shown in Figure 3(top). At later times, our bed mechanics model slightly improves model-and-experiment agreement over the constant permeability model. In Figure 3 (bottom), we see that accounting for spatial variations of the permeability has a negligible effect on the reactor temperature response.

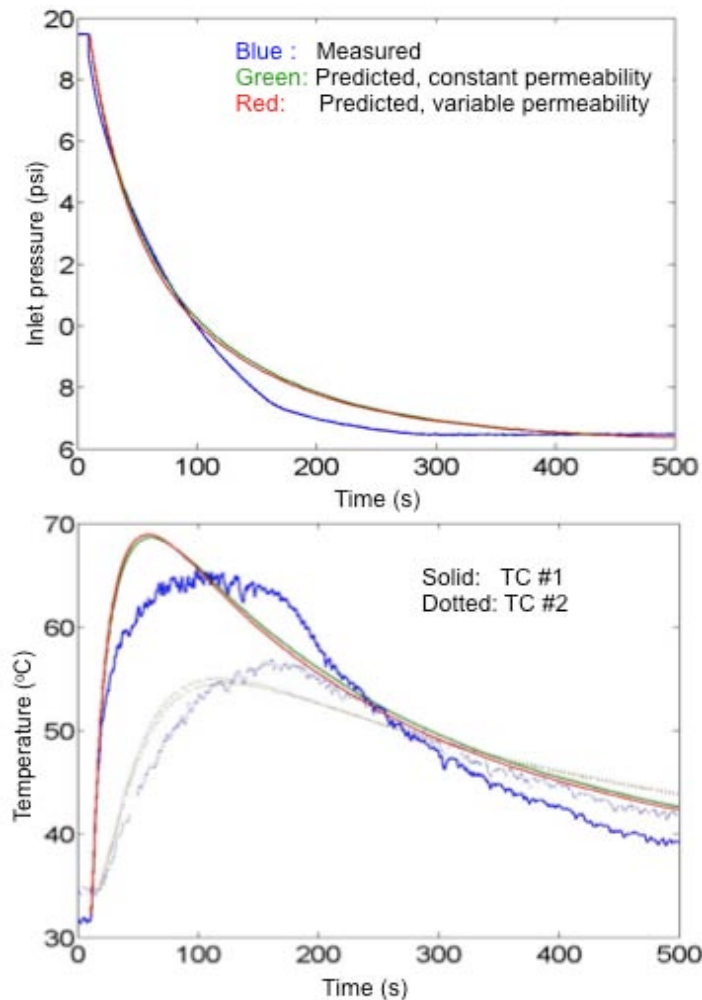


Figure 3: Measured and predicted pressure decay in the O₂ source vessel, (top), and temperatures at TC #1 and TC #2, (bottom). Here we compare the experimental results with predictions from Kanouff et al.'s constant permeability model and our variable permeability model.

O₂ injection #2

In this experiment, the O₂ source bottle had a higher initial pressure, 52 psia, and therefore oxygen flowed into the bed more rapidly. Approximately 36% of the bed was oxidized after 500 s. Consequently, heat is generated more rapidly, which leads to higher temperatures (see Figure 4(a)). For much of the injection, local temperatures are high enough to decompose UD₃ and produce U, as shown in Figure 4(b). Thermal and phase expansions are more

pronounced in this case, leading to larger changes in porosity and permeability near the reaction front. We also find that regions downstream of the front experience higher compression stresses, which decrease their porosity and permeability (Figure 4(c-d)). In this case, porosity and permeability in the downstream regions are decreased to about 0.54 and 3×10^{-10} cm² respectively; whereas in O₂ injection #1, they were about 0.59 and 6×10^{-10} cm² respectively. These highly non-uniform porosity and permeability fields significantly impact the pressure and temperature response of the reactor.

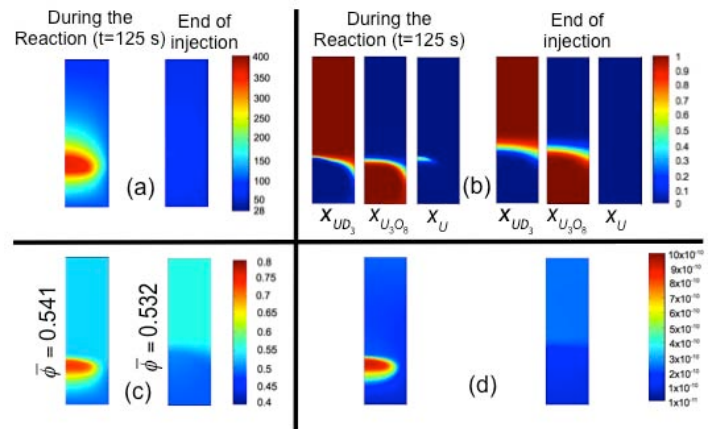


Figure 4: Plots of the (a) temperature (°C), (b) composition, (c) porosity, and (d) permeability (cm²), inside the bed for O₂ injection #2. The plots are generated during the reaction (t=125 s) and at the end of the injection, as indicated.

Figure 5(top) shows the measured O₂ source-volume pressure along with model predictions. We see that including detailed bed mechanics significantly improves the pressure prediction. This is largely because the solid mechanics model more accurately describes the porosity and permeability changes during oxygen injection. Knowledge of the spatially varying permeability gives better knowledge of the overall bed permeability.

Including bed mechanics also improves the temperature prediction. Because the varying oxygen injection rate is captured more accurately, the heat generation rate is more accurately modeled; and therefore the maximum reactor surface temperatures are predicted with greater accuracy. Despite the improvements brought by the solid mechanics model, significant disagreement still exists in the reactor surface temperature response. This may be due to our lack of a truly quantitative model for UD₃ oxidation kinetics. As direct oxidation of uranium hydride has received very little attention in the literature, we are using kinetic expressions given in (8-9), which were determined by fitting to similar oxygen injection experiments. Additional experiments are needed to validate, and perhaps improve, the UD₃ oxidation rate model.

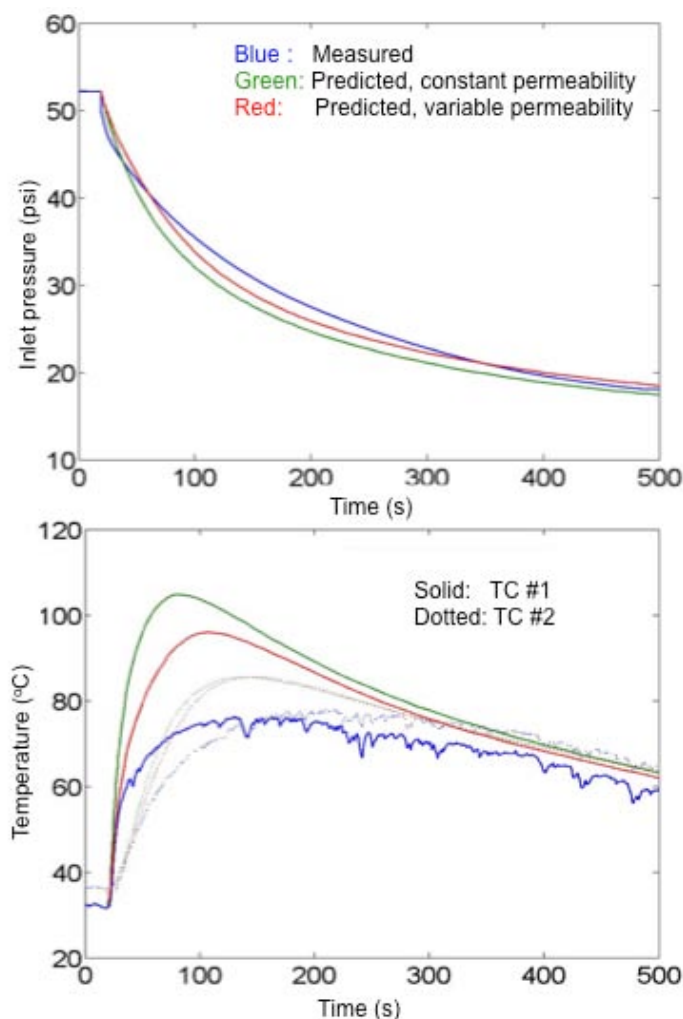


Figure 5: The measured and predicted (top) pressure decay in the O_2 source vessel, (bottom) temperatures at the locations of thermocouples TC #1 and TC #2, as indicated. The predictions were obtained using the constant permeability model of Kanouff *et.al.* (9) and the current variable permeability model for O_2 injection #2.

CONCLUSION

In this paper, a simplified solid mechanics model of packed bed deformation was coupled to an existing multiphysics finite element model for the reaction of oxygen gas and uranium hydride within a hydrogen storage bed. This extended model was applied to two oxygen injection cases, and the predictions were compared to experimental measurements. It was found that accounting for the internal bed deformations by using a coupled solid mechanics model enables a more accurate quantification of the bed permeability. For low rates of oxygen injection, where the chemical reactions are limited to uranium hydride oxidation, accounting for the bed mechanics does not have a significant effect on the pressure and temperature responses of the uranium hydride reactor bed. However, for higher injection rates where significant heating and uranium

hydride decomposition both occur, the bed mechanics model improves model-and-experiment agreement. The agreement is far from perfect however and more experimental and theoretical work is needed to better understand the reactor response.

ACKNOWLEDGMENTS

This work was supported by the Advanced Simulation and Computing Physics and Engineering Models (ASC-PEM) programs at Sandia National Laboratories. Sandia National Laboratories is a multi-program laboratory managed and operated by Sandia Corporation, a wholly owned subsidiary of Lockheed Martin Corporation, for the U.S. Department of Energy's National Nuclear Security Administration under contract DE-AC04-94AL85000.

REFERENCES

1. C.C. Bowman and V.A. Vis. Tritium handling facility at KMS fusion inc. *J. Vac. Sci. Tech. A: Vacuum, Surfaces, and Films*, 8(3):2890, 1990.
2. L.K. Heung. Tritium transport vessel using depleted uranium. *Fusion. Tech.*, 28(3):1385, 1995.
3. T. Hayashi *et.al.* Safe handling experience of a tritium storage bed. *Fusion. Eng.Des.*, 83:1429, 2008.
4. T.C. Totemeier. Characterization of uranium corrosion products involved in a uranium hydride pyrophoric event. *J. Nucl. Mat.*, 278(2-3):301, 2000.
5. F. Le Guyadec *et.al.* Pyrophoric behaviour of uranium hydride and uranium powders. *J. Nucl. Mat.*, 396:294, 2010.
6. G.R. Longhurst. Pyrophoricity of tritium-storage bed materials. *Fusion. Tech.*, 14:750, 1988.
7. G.L. Powell. Reaction of oxygen with uranium hydride. In *Advanced Materials for Energy Conversion*, Chandra, 2004.
8. A.D. Shugard, G.M. Buffleben, M.P. Kanouff, S.C. James, D.B. Robinson, B.E. Mills, P.E. Gharagozloo, and P. Van Blarigan. Rapid hydrogen gas generation using reactive thermal decomposition of uranium hydride. Report SAND2011-6939, Sandia National Laboratories, 2011.
9. Kanouff, M.P., Gharagozloo, P.E., Salloum, M., Shugard, A.D. "A Multiphysics Numerical Model of Oxidation and Decomposition in a Uranium Hydride Bed" *Chem. Eng. Sci.* (in press).
10. J.B. Young and B. Todd. Modelling of multi-component gas flows in capillaries and porous solids. *Int. J. Heat. Mass. Trans.*, 48:5338, 2005.
11. E.S. Fischer "Temperature dependence of the elastic moduli in alpha uranium single crystals, part IV (298 K to 923 K)" *J. Nucl. Mat.*, 18:39-54, 1966.
12. T.R.G. Kutty, K.N. Chandrasekharan, J.P. Panakkal and J.K. Ghosh. "Fracture toughness and fracture surface energy of sintered uranium dioxide fuel pellets" *J. Mat. Sci. Lett.*, 6:260-262, 1987.
13. M.O. Marlow "High temperature isothermal elastic moduli of UO_2 " *J. Nucl. Mat.*, 33:242-244, 1969.
14. C.Y. Wu, O.M. Ruddy, A.C. Bentham, B.C. Hancock, S.M. Best, J.A. Elliott. Modelling the mechanical behaviour of pharmaceutical powders during compaction. *Powder Technology*, 152:107-117, 2005.

15 . F.D. Manchester and A. San-Martin “The H-U (Hydrogen-Uranium) System” *J. Phase. Equil.*, 16(3):263-275, 1995.

16 . F.A. Halden, H. C. Wohlers and R.H. Reinhart. “Thermal expansion of uranium dioxide” United States

Atomic Energy Commission, Metallurgy and Materials Branch, Washington D.C., April 1959.

17 . Comsol Multiphysics 3.5a, Solid Mechanics Module User’s Manual, Comsol Inc., 2008.